

Highlights from the Pierre Auger Observatory

M. BOHACOVA⁽¹⁾ ON BEHALF OF THE PIERRE AUGER COLLABORATION⁽²⁾

⁽¹⁾ *Institute of Physics of the Academy of Sciences of the Czech Republic, Na Slovance 2, 182 21 Praha 8, Czech Republic*

⁽²⁾ *Full author list available at: http://www.auger.org/archive/authors_2010-11.html*

Summary. — We present a review of recent results from the Pierre Auger Observatory, including the measurement of the cosmic ray energy spectrum above 10^{18} eV, searches for anisotropy of the arrival directions, and studies of cosmic ray mass composition. The flux exhibits hardening at 4×10^{18} eV followed by suppression consistent with the GZK effect above 3×10^{19} eV. Correlation of cosmic ray air shower arrival directions with the distribution of the nearby extragalactic matter is observed at energies above 5.5×10^{19} eV. The observed longitudinal development of air showers suggests that the interaction cross-section increases with energy more rapidly than current models predict for proton primaries, perhaps due to a transition to heavier composition. No clear candidates for neutrinos and photons in the ultra-high energy cosmic ray flux have yet been found.

PACS 95.55.Vj – 95.85.Ry.

1. – Introduction

The Pierre Auger Observatory [1] was built to study the properties of extensive air showers produced by cosmic rays with energies above 10^{18} eV. It is located in the southern hemisphere near the town of Malargüe, Argentina. The observatory features a large detection area to collect a significant number of rare cosmic ray events. It is the first experiment observing air showers simultaneously by two detection techniques, making it possible to reduce the systematic uncertainties associated with each method. The surface detector (SD) is an array of more than 1600 water Cherenkov detectors sampling the lateral distribution of the shower particles on the ground. The SD has a duty cycle of almost 100%. The fluorescence detector (FD) consists of 27 telescopes observing the longitudinal development of the showers in the atmosphere above the surface array. The light is from nitrogen emission in the near UV region and so the FD can operate only during clear moonless nights, limiting its duty cycle to less than 15% [2]. This technique provides a calorimetric and therefore essentially model-independent measurement of the shower energy, which is used to calibrate the SD measurements. The modular design of the observatory made it possible to start data taking in 2004, before the baseline

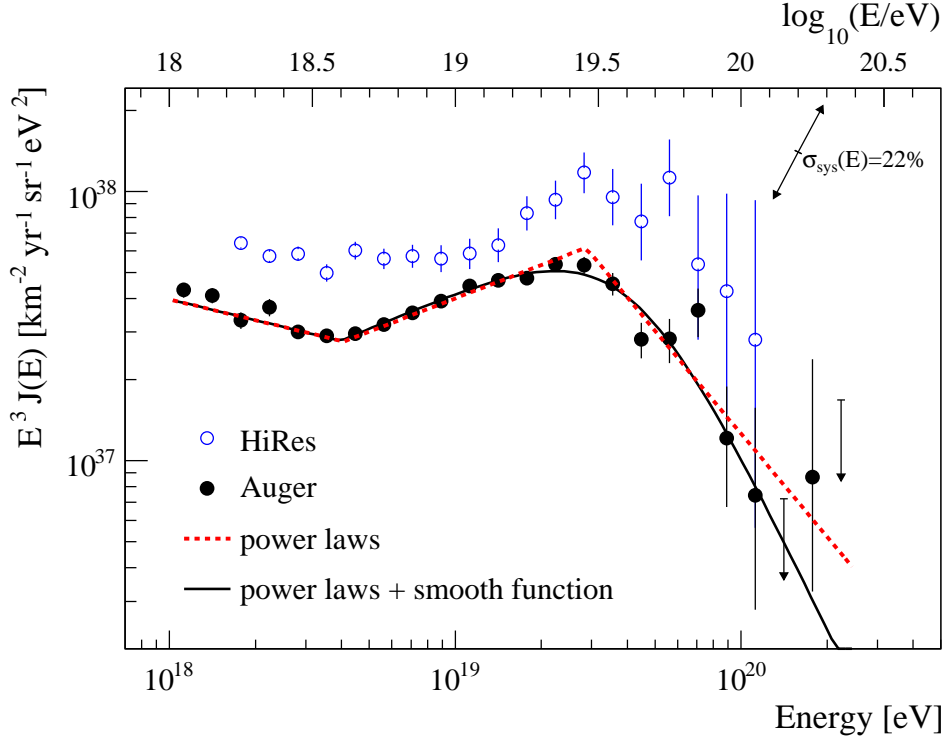


Fig. 1. – Combined hybrid and SD energy spectra from Auger [4] compared to the stereo spectrum from HiRes [5].

configuration was completed in 2008. By the end of 2009 a total exposure of about 20 000 km² sr yr was collected, significantly more than that of all previous air shower experiments combined.

2. – Energy spectrum

Measuring the cosmic ray energy spectrum is a key aspect in understanding the origin and nature of particles whose energies exceed by many orders of magnitude the energy achievable in man-made accelerators. The most direct shower energy determination is obtained by the fluorescence technique. The fluorescence yield (photons emitted per unit of electron energy deposited) characteristics are determined in laboratory measurements [3]. The total energy deposited by the shower is then given by integrating the light observed as the shower develops. A subset of hybrid events (detected by both techniques) are used to establish the relationship between the SD particle density parameter and the FD determined energy. This relation is then used to derive the energy of the full SD data sample. The combined hybrid and SD-only spectrum from the Pierre Auger Observatory is shown in Fig. 1. The spectrum can be described by a broken power-law E^{-s} with the spectral index $s = 3.26 \pm 0.04$ below the first break located at $\log(E) = 18.61 \pm 0.01$ (called the ankle). The spectral index reaches 2.59 ± 0.02 above the ankle and then steepens again to $s = 4.3 \pm 0.2$ above the second spectral feature at $\log(E) = 19.46 \pm 0.03$. The HiRes stereo spectrum is shown for comparison. The apparent overall shift of the

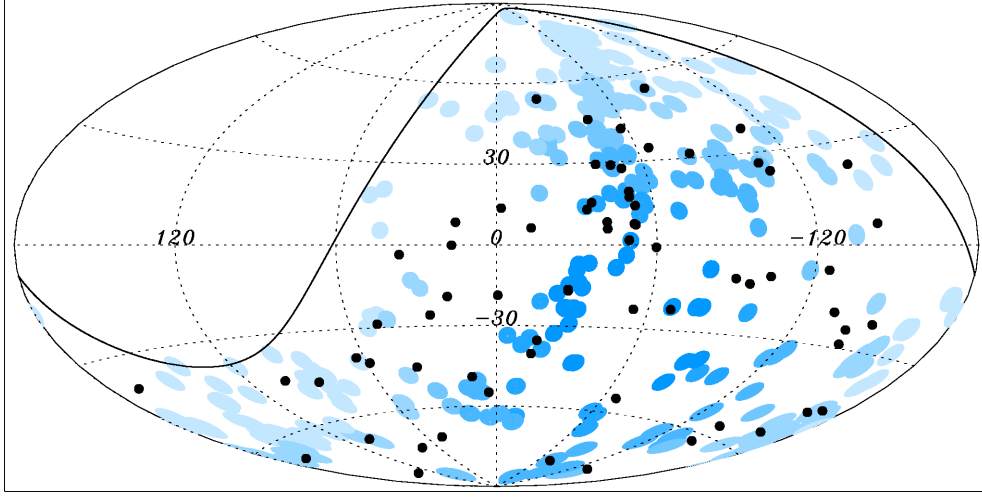


Fig. 2. – Arrival directions of the 69 events above 55 EeV (dots). The circles of 3.1° are centered around the positions of the 318 AGNs from the VCV catalog that are located within 75 Mpc distance and within the field of view of the observatory (solid curve). The shading of the circles indicates the relative exposure at these locations. Cen A is located at $l \sim -50.5^\circ$, $b \sim 19.4^\circ$.

two spectra is not yet understood, but they are consistent within systematic errors [4] (about 20 % for each experiment).

Although the observed features are consistent with the GZK predictions (for proton dominated composition), one should realize that this does not necessarily mean that this is in fact the mechanism behind the suppression. For example it is also conceivable that the suppression is caused by the maximum energy achievable by the cosmic accelerators. Interpretation of the spectral features should be done using also the information from chemical composition studies and searches for photons and neutrinos. The ankle may be a result of a steep spectrum from galactic sources crossing over a flatter spectrum from the extragalactic sources.

3. – Arrival directions

With increasing energy the trajectories of cosmic ray particles become less deflected in the galactic and extragalactic magnetic fields, giving hope that astronomy at ultrahigh energies will become feasible. Moreover, if the observed flux suppression is the GZK effect, then 10^{20} eV particles can not reach the Earth from distances of order 100 Mpc or beyond. Since nearby extragalactic matter is not uniformly distributed, these facts motivate a search for anisotropy in the arrival directions of cosmic rays. One class of objects believed capable of accelerating particles to ultrahigh energies are Active Galactic Nuclei (AGN). The Pierre Auger Collaboration found a significant correlation with objects from the Véron-Cetty & Véron catalog [9], the effect appearing for events with energy above 55 EeV, angular separation from catalog objects of less than 3.1° , and for AGNs less than 75 Mpc distant [6].

An update of the fraction of correlating events detected until 31 December 2009 excluding the 14 initial events used to establish the hypothesis, yields $38^{+7}_{-6}\%$, where only 21 % would be expected for an isotropic distribution [7]. The 69 events with energies

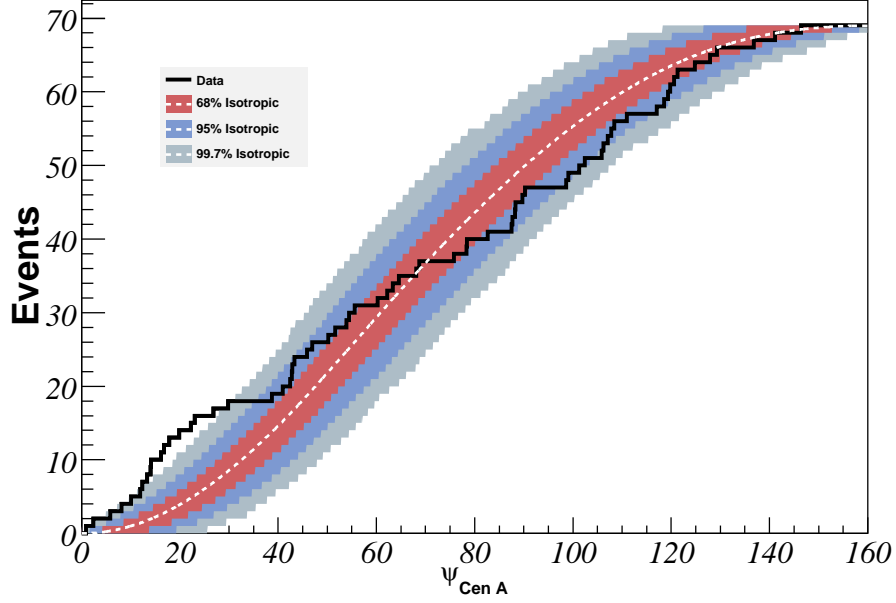


Fig. 3. – Cumulative number of events with $E \geq 55$ EeV as a function of angular distance from the direction of Cen A. The bands correspond to 68 %, 95 %, and 99.7 % dispersion expected for an isotropic flux.

above 55 EeV detected in this time period are plotted in Fig. 2. Note that the catalogs are incomplete near the galactic plane due to obscuration, so the lack of correlation for events in this region is expected. Details of these studies are reported in [7].

Especially interesting is the concentration of events around the location of Centaurus A, which lies only ~ 4 Mpc away from us. Plotting the number of observed events as a function of angular distance from Cen A shows the most significant excess for events within 18° , where 13 events were observed while only 3 are expected for an isotropic distribution (Fig. 3). It is unclear whether the events come from the Cen A nucleus, its radio lobes, or even from other objects, perhaps in the Centaurus galaxy cluster, located about 45 Mpc behind Cen A on the same line of sight. Of course, the possibility that the excess could be a random fluctuation has not yet been ruled out.

4. – Mass composition

Information about the mass and type of the primary particle is another key component in understanding the origin of ultra-high energy cosmic rays. The chemical composition of the primaries will affect the resulting air showers most significantly in the electron/muon ratios at the ground level and the depth-of-maxima in the atmosphere. A simple superposition principle gives some guidance: it approximates an interaction of a nucleus of mass A and energy E as the superposition of A nucleons each with the energy E/A . Hence, for a given energy a proton primary will penetrate deeper into the atmosphere and the shower-to-shower fluctuations will be larger than in the case of a heavier nucleus. Results

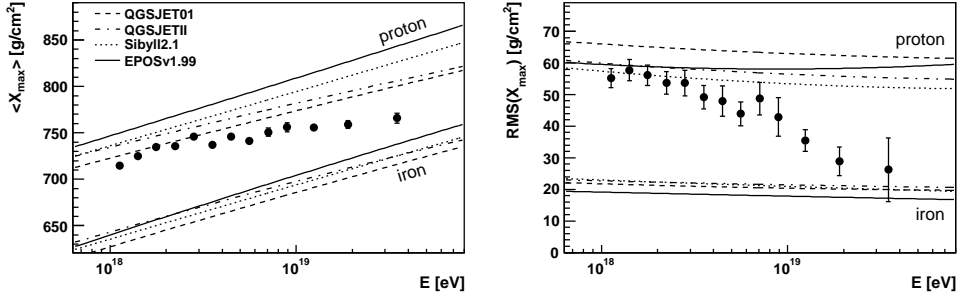


Fig. 4. – Distributions of X_{\max} (left) and $\text{RMS}(X_{\max})$ as a function of energy. Sample contains well-reconstructed hybrid events only. Monte Carlo simulations using different hadronic interaction models are shown for protons and iron nuclei.

of the studies of the X_{\max} distribution and its RMS are presented in Fig. 4 together with predictions for a pure proton and a pure iron composition from various hadronic interaction models. Further details of this analysis can be found in [8]. It is necessary to invoke hadronic physics models to assess the composition, but there are no models that properly represent all observed air shower characteristics. Thus it is dangerous to make inferences using them. Current models are extrapolating the features of the hadronic interactions well beyond the region tested by accelerator data. Consequently, the systematic uncertainties of the predictions are significant. With these caveats in mind, both $\langle X_{\max} \rangle$ and $\text{RMS}(X_{\max})$ suggest a trend from a lighter composition to heavier (*e.g.* CNO). The trend coincides with the position of the ankle in the spectrum. Only the highest quality events detected by the FD are considered in this study, limiting the number of events analyzed. An unfortunate result is that the statistics do not yet allow extension of this analysis to the highest energies, where the correlations with AGNs are observed. Reconciling this composition trend with the observed anisotropy may be very challenging.

It is interesting to note that an increase in the proton-nucleus inelastic cross-section at the highest energies would bring model predictions for protons closer to the data by making X_{\max} higher in the atmosphere. Results from the LHC, particularly in the forward region, will be of great interest for the cosmic ray community as they are expected to improve the reliability of the hadronic interaction models.

Independently of the LHC experiments (and at energies beyond their reach), the Pierre Auger Observatory can investigate some aspects of hadronic interaction models. For example, several examinations of the intensity of the muon component in extensive air showers have been performed, with preliminary results suggesting that showers contain more muons than the models predict[10].

5. – Photon and neutrino limits

Photons and earth-skimming neutrinos are expected to have a characteristic signature in the data, since both produce showers that develop deep in the atmosphere. Both kinds will be seen as young showers, while an earth-skimming tau neutrino will also have a nearly horizontal trajectory. Searches for such events have yielded strong limits that exclude some of the so-called 'exotic scenarios' for the production of ultra-high energy cosmic rays. The current upper limit from the Auger data for the fraction of photons in

the UHECR flux is 2% above 10 EeV and 2.4% above 2 EeV [11]. For the tau neutrino flux in the energy range $2 \times 10^{17} \text{ eV} < E_\nu < 2 \times 10^{19} \text{ eV}$, assuming a diffuse spectrum of the form E_ν^{-2} the corresponding upper limit is $6 \times 10^{-8} \text{ GeV cm}^{-2} \text{ s}^{-1} \text{ sr}^{-1}$ [12].

6. – Observatory enhancements

The Pierre Auger Observatory is now collecting around $7000 \text{ km}^2 \text{ sr}$ of exposure per year. New detector systems are being deployed now to compare our measurements with other experiments working at lower energy. HEAT (High Elevation Auger Telescopes) has three telescopes with their field of view pointing above the baseline Auger instruments, allowing observation of nearby lower energy showers ($\gtrsim 10^{17} \text{ eV}$) [13]. AMIGA (Auger Muon and Infill for the Ground Array) is essentially a denser grid of surface stations paired with underground muon counters and will perform a precise study of the lateral shower profile as well as the muon content in the energy region between 10^{17} eV and 10^{19} eV [14]. AERA (Auger Engineering Radio Array) is exploiting yet another detection technique, the measurement of the coherent radiation at radio frequencies emitted by secondary shower particles deflected in the geomagnetic field [15].

As the new devices are put to operation and the analysis of new data is ongoing, more interesting results can be expected.

* * *

The contribution was prepared with the support of Ministry of Education, Youth and Sports of the Czech Republic within the project LA08016.

REFERENCES

- [1] J. ABRAHAM ET AL. [PIERRE AUGER COLL.], *Nucl. Instr. Meth.*, **A523** (2004) 50.
- [2] J. ABRAHAM ET AL. [PIERRE AUGER COLL.], *Nucl. Instr. Meth.*, **A620** (2010) 227-251
- [3] SEVERAL PAPERS, *Nucl. Instr. Meth.*, **A597** (2008) .
- [4] J. ABRAHAM ET AL. [PIERRE AUGER COLL.], *Phys. Lett. B*, **685** (2010) 239-246
- [5] R. ABBASI ET AL. [HIRES COLLABORATION], *Astropart. Phys.*, **32** (2009) 53
- [6] J. ABRAHAM ET AL. [PIERRE AUGER COLL.], *Science*, **318** (2007) 938; *Astropart. Phys.*, **29** (2008) 188
- [7] R. ABREU ET AL. [PIERRE AUGER COLL.], *Astropart. Phys.*, **34** (2010) 314
- [8] J. ABRAHAM ET AL. [PIERRE AUGER COLL.], *Phys. Rev. Lett.*, **104** (2010) 091101
- [9] M.-P. VÉRON-CETTY AND P. VÉRON, *A&A*, **455** (2006) 773-777
- [10] A. CASTELLINA FOR THE PIERRE AUGER COLL., *Proc. 31st ICRC(Lodz, Poland)*, (2009) 0033
- [11] J. ABRAHAM ET AL. [PIERRE AUGER COLL.], *Astropart. Phys.*, **31** (2009) 399
- [12] J. ABRAHAM ET AL. [PIERRE AUGER COLL.], *Phys. Rev. D*, **79** (2009) 102001
- [13] M. KLEIFGES FOR THE PIERRE AUGER COLL., *Proc. 31st ICRC(Lodz, Poland)*, (2009) 0410
- [14] A. ETCHEGOYEN FOR THE PIERRE AUGER COLL., *Proc. 30th ICRC(Mérida, Mexico)*, (2007) 1307
- [15] A.M. VAN DER BERG FOR THE PIERRE AUGER COLL., *Proc. 31st ICRC(Lodz, Poland)*, (2009) 0232